

## THE PROTECTION OF ALLOYS AGAINST HIGH TEMPERATURE SULPHIDATION BY $\text{SiO}_2$ -COATINGS DEPOSITED BY MOCVD

R. Hofman, J.G.F. Westheim, T. Fransen, and P.J. Gellings  
*Laboratory for Inorganic Chemistry, Department of Chemical Technology  
University of Twente, P.O.Box 217, 7500 AE Enschede  
The Netherlands*

### ABSTRACT

Silica coatings have been deposited on various alloys by MOCVD (Metal Organic Chemical Vapor Deposition) to protect them against high temperature corrosion in coal gasification environments. DiAcetoxyDitertiaryButoxySilane (DADBS) has been used as a metal organic precursor at deposition temperatures between 773 - 873 °K and amorphous layers were produced with a growth rate of about  $1 \mu\text{m} \cdot \text{h}^{-1}$ . These coatings have been tested at 823°K in a sulphidizing atmosphere with a low oxygen ( $9.3 \times 10^{-29}$  bar) and a high sulphur partial pressure ( $1.2 \times 10^{-9}$  bar). In this environment the sulphidation resistance of various alloys has improved by a factor of at least 100 by the coating. The observed corrosion reaction is local and is explained by a model in which in the first stage cracks are formed due to mechanical stresses in the coating. In the second stage metal sulphides are formed by outward diffusion of metal and inward diffusion of sulphur through the cracks. When stainless steels are used as the alloy the outer layer consists of FeS and the lower one of CrS.

### INTRODUCTION

In recent years ceramic coatings have been used to improve the wear resistance and the corrosion resistance of bulk materials. The required layer thickness of these coatings varies from a few atomic layers to several microns and consequently different techniques have been used to deposit these coatings: Plasma spraying, PVD, (MO)CVD and sol-gel. Next to the thickness range also a wide variety of oxide-ceramics, e.g.,  $\text{Al}_2\text{O}_3$ ,  $\text{ZrO}_2$  and  $\text{SiO}_2$  and non oxide-ceramics, e.g., TiN, SiC and  $\text{Si}_3\text{N}_4$ , have been deposited on many different substrates.

The protection of alloys against high temperature corrosion is mostly obtained by oxidation. In coal gasification environments, i.e., a gas environment with a low oxygen and a high sulfur pressure, often ceramic or metallic coatings have been used to protect metal parts. Coating technology in this area is based on pack cementation (1) and plasma spraying (2), while only few authors report MOCVD (3), PACVD (4) and PVD techniques to protect the alloys against this type of corrosion. Regarding MOCVD only Morssinkhof et al.(3) have used a technique to deposit amorphous  $\text{Al}_2\text{O}_3$ . The metal organic precursor used in their work was Aluminum Tri Isopropoxide and deposition temperatures between 523 to 723 °K were necessary to obtain protective coatings. Coley et al. (4) used a PACVD technique to deposit amorphous  $\text{SiO}_2$  coatings to reduce the oxidation rate of alloys between 1000°K and 1300°K. At these temperatures they found the degradation of the coatings to be due to crystallization of the coatings and solid state reactions between the coating and the metal. Fortunately, metal parts of the coal gasification equipment are exposed to lower temperatures (about 773°K) and this type of degradation will not be observed.

The coating failure, in general, is linked to the process by which the coating is applied (e.g., formation of porous or cracked coatings), its compatibility with the substrate (e.g., due to different thermal expansion coefficients) and the response of the coating to its environment (e.g., corrosion of the coating) (5). Since reaction of  $\text{SiO}_2$ -coatings with the used environment is thermodynamically impossible, degradation will only take place by diffusion of sulphur through coating defects, induced either by the deposition process or by a thermal mismatch between the ceramic coating and the substrate, and a subsequent reaction of sulphur with the alloy. The mechanism of the reactions of sulphur with the alloy through coating defects is in principal identical to that of uncoated metals, as reviewed by Gesmundo (6).

In the present work a MOCVD-technique is described to deposit coatings at low temperatures to avoid phase transitions and diffusion in the metals. This low deposition temperature is possible, when DiAcetoxyDitertiaryButoxySilane (DADBS) is used instead of the more familiar Tetra EthOxy Silane (TEOS) (7).

## EXPERIMENTAL

In Fig.1 a schematic drawing of the MOCVD equipment is presented. The metal organic precursor DADBS (DiAcetoxyDitertiaryButoxySilane/Petrarch) is kept at a constant temperature in a saturator vessel. Through this saturator nitrogen gas is passed to create the desired vapor. The DADBS concentration in the vapor phase can be reduced by mixing the gas stream from the saturator by an extra amount of nitrogen gas. The furnace temperature is controlled by a thermocouple to which the sample is mounted. The used deposition parameters, unless stated otherwise, were kept constant. The temperature of the oil bath, used to heat the DADBS saturator, was 353°K, the gas flow through the DADBS was 24 l.h<sup>-1</sup>, the diluting gas flow was 24 l.h<sup>-1</sup>, the reactor pressure was always 1 atm. and the reaction temperature was

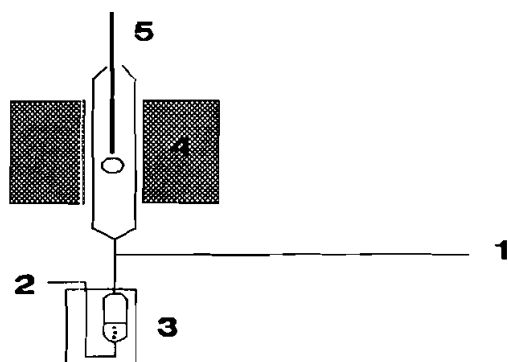


Figure 1. Schematic presentation of the MOCVD equipment. 1 = diluting gas stream, 2 = carrier gas stream, 3 = DADBS saturator, 4 = furnace, 5 = thermocouple with specimen.

833°K. The composition of the gas outlet was recorded by a mass spectrometer (Masspec) to study the reaction mechanism.

The alloys that have been coated, were AISI 304, AISI 321, Incoloy 800H and AISI 310 of which the composition is given in Table 1. Prior to the deposition the specimens were polished on 25, 6, 1 and 0.25  $\mu\text{m}$  diamond paste and finally etched in a solution of 95% ethanol (p.a.), 5% 3 M nitric acid.

Table 1  
The nominal composition of the used alloys  
in percent. All the alloys are iron based and the  
silicon and carbon content are the maximum amounts.

Alloy	Cr	Ni	Mn	Si	Ti	C
AISI 304	19	9	2.0	1.0	--	0.08
AISI 310	25	20	2.0	1.5	--	0.25
AISI 321	18	10	2.0	1.0	0.4	0.1
INCOLOY 800H	19.9	31.7	0.7	0.5	0.7	0.08

Both coated and uncoated specimens have been tested in a 1%  $\text{H}_2\text{S}$ , 1.5%  $\text{H}_2\text{O}$ , 19%  $\text{H}_2$ , Ar (bal.) gas mixture at 823°K. The resulting partial oxygen ( $\text{O}_2$ ) pressure in this gas mixture was  $9.3 \times 10^{-23}$  bar at 823°K, while the partial sulphur ( $\text{S}_2$ ) pressure was  $1.2 \times 10^{-9}$  bar. These conditions are used to simulate coal gasification environments. The weight gain of the specimens due to the corrosion reaction of the

specimens with the gas mixture were recorded by a spring balance (see Fig.2). The specimens were mounted to the spring by a platinum wire and hanged in the furnace, which was kept at 823°K. A black plate situated between the spring and the specimen intercepts a laser beam and consequently the measured light intensity by the receiver is less than the emitted intensity. When the weight of the specimen increases, the spring elongates, the laser beam is less intercepted and the measured light intensity becomes higher. For small elongation differences the measured light intensity is a linear function of the weight gain and measured continuously by a computer. The elongation coefficient of the spring is a function of the temperature and the spring therefore is kept at  $323.0 \pm 0.1^\circ\text{K}$ . At this temperature the spring did not degrade. The accuracy of the spring balance is 0.01 mg.

Cyclic oxidation experiments have been performed in air between room temperature and 1123°K. The heating rate was  $60^\circ\text{K}\cdot\text{h}^{-1}$ , the cooling rate  $30^\circ\text{K}\cdot\text{h}^{-1}$ , while the specimens were held for 24 h. or 48 h. at the highest temperature.

Surface morphology and cross sections of the specimens were examined by SEM/EDX (JEOL/KEVEX), while the formed sulphide phases were analyzed by XRD.

## RESULTS AND DISCUSSION

The decomposition of DADBS as a function of the reaction temperature was analyzed by a mass spectrometer. The results of these measurements are shown in Fig.3. In Table 2 the peaks with the highest intensity of the scanned elements are given. The partial pressure of acetic acid ( $M/e = 60$ ) and 2-methyl propanol were also recorded, but never exceeded the detection limit. From these results it can be concluded that the decomposition of DADBS takes place in several steps and that

Table 2  
The scanned mass spectroscopic peaks of several compounds.

Compound	1st Peak (M/e)	2nd Peak (M/e)	3rd Peak (M/e)
2-methyl propene	41	56	55
2-methyl propanol	59	41	31
Acetic acid	43	60	44
Acetic acid anhydride	43	42	44

For acetic acid the peak of  $M/e = 60$  has been recorded, to prevent interference with the peaks of acetic acid anhydride.

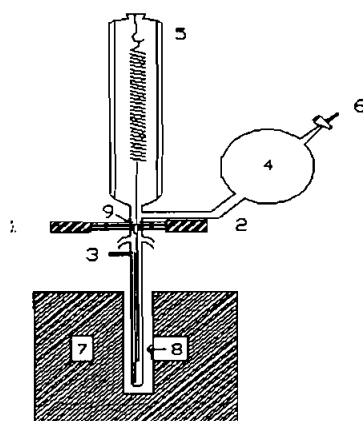


Figure 2. Schematic representation of the spring balance. 1,2 = laser transmitter and receiver, 3,6 = gas in and outlet, 4 = gas reservoir, 5 = spring, 7 = furnace, 8 = specimen and 9 = laser beam interceptor.

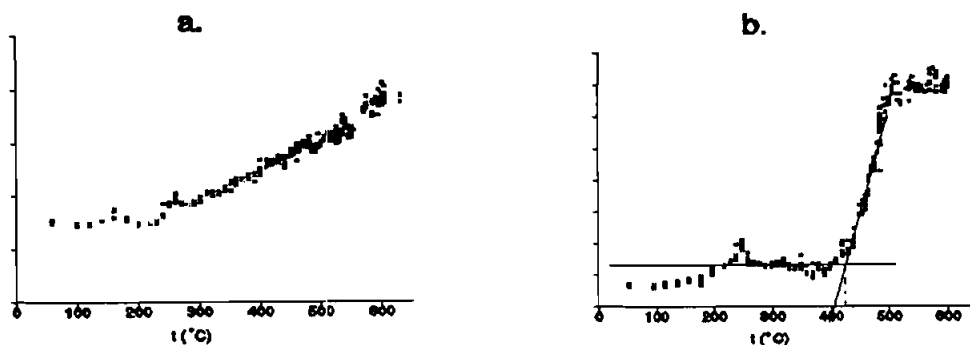


Figure 3. The measured relative pressure of acetic acid anhydride (a) and 2-methyl propene (b) as a function of reaction temperature of DADBS.

2-methyl propanol and acetic acid are not formed. In the first step acetic acid anhydride is formed at 473°K, while a temperature of 673°K is required to form 2-methyl propene. The remaining silicon hydroxide is finally transformed to amorphous silica through a polycondensation reaction. According to this mechanism no  $\text{SiO}_2$  will be formed at temperatures below 673°K, which is in accordance with experiments. A more detailed decomposition mechanism is described elsewhere (8).

The observed reaction rate varies from 0.12 at 773°K to  $1.2 \mu\text{m}\cdot\text{h}^{-1}$  at 873°K. At high temperatures the reaction rate will be controlled by a diffusion process of reactants and by-products through a diffusion layer. In this diffusion-controlled regime porous films are formed and the metals will not be protected against

corrosion. In the reaction-controlled regime (at low temperatures), the alloys will become homogeneously coated. From Fig.4 both the diffusion controlled and the reaction controlled regime can be observed and the activation energy of the decomposition reaction is  $155 \text{ kJ.mole}^{-1}$ .

The sulphidation resistance of AISI 321 is improved by a factor of at least 100 by amorphous silica coatings as can be seen from Fig.5. The amorphous silica coating does not react with the  $\text{H}_2\text{S}$ , but degradation of the metal takes place through pores and cracks in the coating as seen in Fig.6. Weight losses due to spallation of the sulphide scale, which is expected for thick scales, has not been observed in agreement with the morphology of the corrosion products and the coatings. The observed local degradation of the coated systems consists of two semicircular product layers: one on the coating and one under the coating. The outer product layer is a multicomponent chromium and iron sulphide scale, in which the iron content increases from the coating/metal interface to the gas/oxide interface. The inner layer is always a chromium sulphide scale (see Fig.7).

The observed degradation can be explained by a two step model (see Fig.8) in the coating. These can be due to thermal mismatch between the ceramic coating and the alloys. Thermal stresses in the coatings can be calculated with equation (1) and can exceed 1 GPa for ceramic/metal systems (9).

$$\sigma_{\text{ox}} = E_{\text{ox}} \Delta\alpha \Delta T \quad (1)$$

For metal ( $\alpha \approx 14 \cdot 10^{-6} \text{ K}^{-1}$ )/  $\text{SiO}_2$  systems ( $\alpha = 0.5 \cdot 10^{-6} \text{ K}^{-1}$  and  $E = 75 \text{ GPa}$ ) the calculated stress is 0.54 GPa.

In the second step, once cracks penetrating the coating have been formed, sulphur from the gas will diffuse through the cracks and react with metal to form metal sulphides. After a short period the crack will become filled by metal sulphides and a sulphide duct is formed from the alloy to the oxide-gas interface.

The inner product layer, formed by inward diffusion of sulphur, is a CrS scale, while the outward growing layer is a FeS scale, in which Fe diffuses outward. In the used gas environment FeS is a stable phase as can be concluded from the stability diagram of Fe (Fig.9).

In the first stages of scale formation the outward growing scale consists of metastable CrS, which can be explained by the kinetic boundary theory, implying that in practice the  $\text{Cr}_2\text{O}_3/\text{CrS}$  equilibrium line is shifted to a higher oxygen pressure (11) (see Fig.9). This means that in coal gasification environments always CrS is formed instead of  $\text{Cr}_2\text{O}_3$ . Due to the fact that the diffusivity of Fe in CrS is higher than that of Cr in CrS, after a short period  $\text{Fe}_{1-x}\text{S}$  is formed, as confirmed by XRD-analysis.

The above model predicts thinner coatings to be better protective, because thicker coatings will show more cracks due to the stresses in this coating. However, from Fig.5 one could conclude that thinner coatings are less protective than thicker

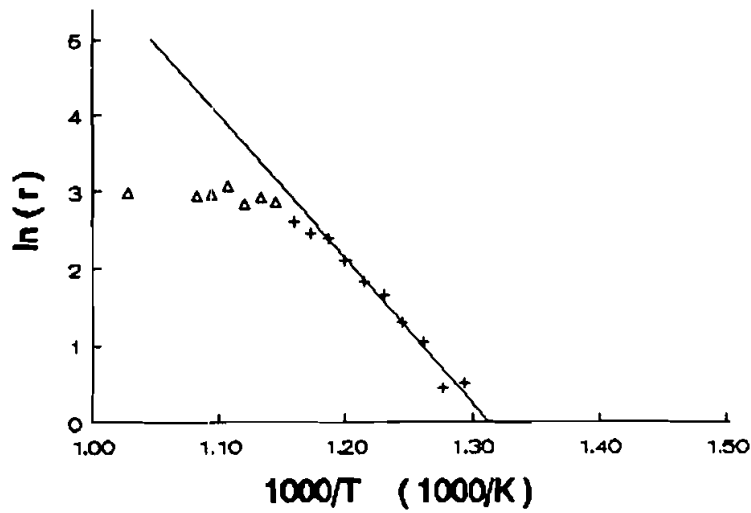


Figure 4. The reaction rate of the decomposition of DADBS as a function of the reaction temperature in an Arrhenius plot.  $\Delta$  = diffusion controlled regime and + = reaction controlled ( $E_{act} = 155 \text{ kJ.mole}^{-1}$ ).

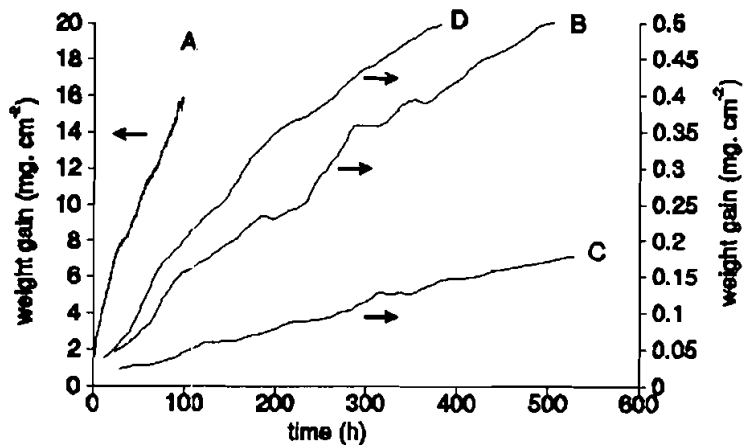


Figure 5. In the first step cracks are formed, due to mechanical stresses The weight gain of AISI 321 specimens during sulphidation in a 1%  $\text{H}_2\text{S}$ , 1.5%  $\text{H}_2\text{O}$ , 19%  $\text{H}_2$ , Ar (bal.) gas mixture at 823°K. A = uncoated, B = 0.66  $\mu\text{m}$   $\text{SiO}_2$  coating, C = 1.12  $\mu\text{m}$   $\text{SiO}_2$  coating, D = 1.63  $\mu\text{m}$   $\text{SiO}_2$  coating.

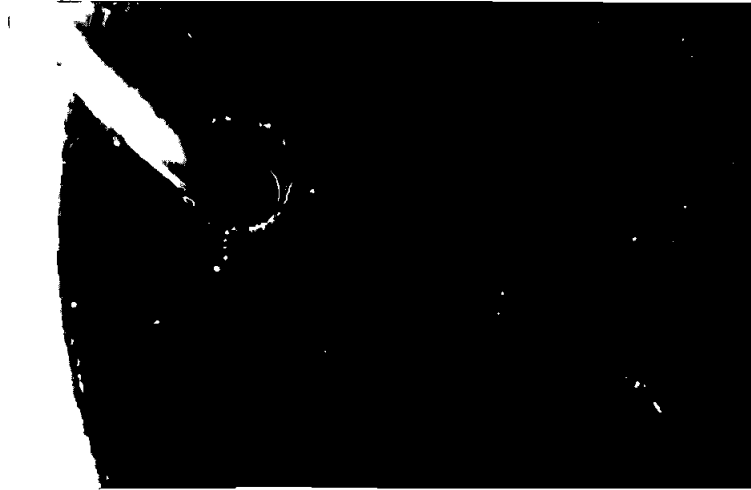


Figure 6. A sulphidized  $\text{SiO}_2$  coated AISI 321 specimen, which is only localized degraded.

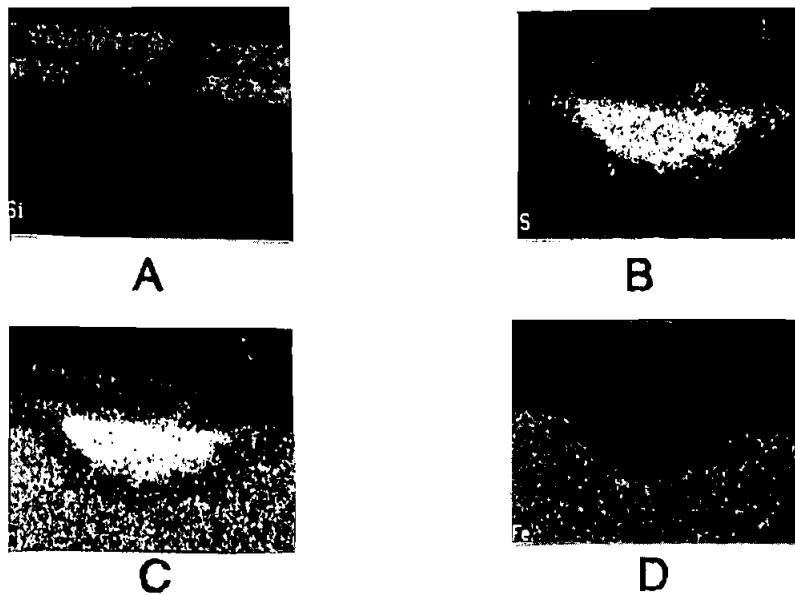


Figure 7. EDX- analysis of a cross section of a sulphidized specimen, in which the inner semicircle and the crack in the coating can be seen. A = Silicon, B = Sulphur, C = Chromium and D = Iron Sulphidation may take place by sulphur and/or metal transport through the sulphide ducts (10).



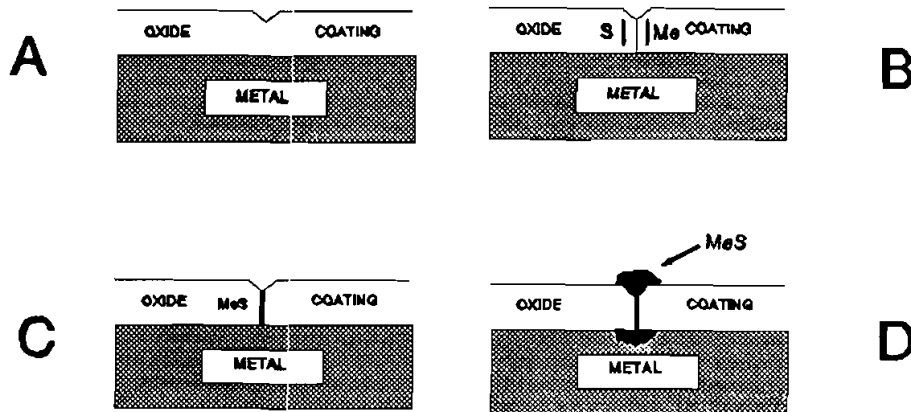


Figure 8. The degradation model of  $\text{SiO}_2$ -coated alloys. The first stages represent crack formation (A). Once penetrating cracks are formed in- and outward diffusion of sulphur and metal ions is possible (B). After a period the crack becomes filled with metalsulphides and a sulphide duct is formed (C). Through this sulphide duct further diffusion of sulphur and metal ions is possible (D).

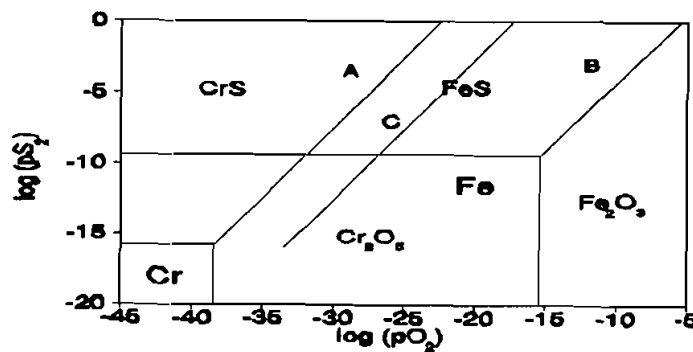


Figure 9. Thermodynamic stability diagram of iron (A) and chromium (B) as function of the oxygen and sulfur partial pressure. Formation of metastable  $\text{CrS}$  is often explained by the kinetic boundary, which means that the  $\text{Cr}_2\text{O}_3/\text{CrS}$  line is shifted towards a higher partial oxygen pressure (C).

coatings. Optical observations (see Fig.10) show that thinner coatings are only attacked at the specimen edges. This phenomenon is due to the gas flow pattern around the specimens during deposition. As a consequence, the growth rate of the

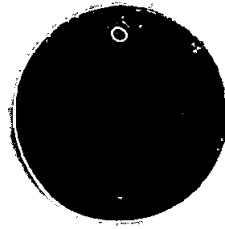


Figure 10. A micrograph of the specimen with a thin coating ( $0.66 \mu\text{m}$ ), which is only degraded at the edges.

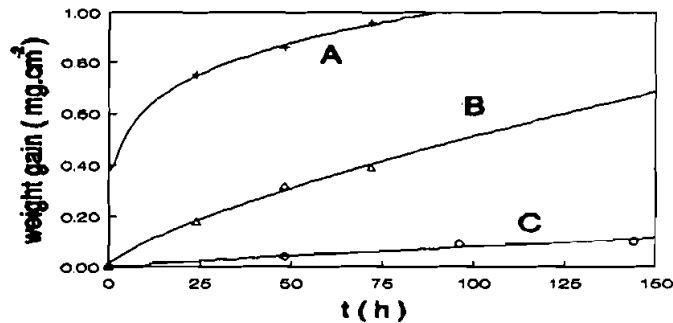


Figure 11. Cyclic oxidation experiments at  $1123^\circ\text{K}$  show that the cyclic oxidation resistance of Incoloy 800H has improved by a  $\text{SiO}_2$  coating. (A = uncoated Incoloy 800H, B =  $0.35 \mu\text{m}$   $\text{SiO}_2$  coating on Incoloy 800H and C =  $2.93 \mu\text{m}$   $\text{SiO}_2$  coating on Incoloy 800H)

oxide layer at edges of the specimens is lower than the overall growth rate and for samples with a thin coating the layers formed at the edges are not closed and a rapid sulphidation is observed. With increasing overall layer thickness the edges will become covered by a closed layer and consequently no sulphidation is observed at these places. Preliminary results with specimens which have a higher surface area indeed show a better sulphidation resistance. It should be pointed out that thicker coatings are preferable to avoid erosion of this coating and the optimum coating thickness should be a compromise between erosion and corrosion properties.

Some experiments have been performed to check the cyclic oxidation resistance of  $\text{SiO}_2$  coatings deposited on Incoloy 800 H between room temperature and  $1123^\circ\text{K}$ , as is described in the experimental section. The results of these experiments (Fig.11) show that resistance of the coated Incoloy 800 H specimens against cyclic oxidation is excellent.

## CONCLUSIONS

MOCVD-layers have been deposited on several alloys by a multi-step reaction mechanism in which acetic acid anhydride and 2-methyl propene are formed. Reasonable reaction rates are obtained in the temperature range 800-873°K. The activation energy of the deposition reaction is found to be 155 kJ.mole<sup>-1</sup>. The sulphidation resistance at 823°K of different alloys is improved by a factor of at least 100 by the deposited amorphous SiO<sub>2</sub> coatings. The observed corrosion reactions are local and can be described by a model in which as a first step cracks in the coating are formed due to mechanical stresses. In the second step metal sulphides are formed by in- and outward diffusion of metal and sulphur. The outward grown layer is FeS, while the inward growing layer is CrS.

## ACKNOWLEDGEMENTS

This research was supported by the Technology Foundation (STW). The authors wish to thank dr. V.T. Zaspalis for providing the analysis equipment (mass spectrometer).

## REFERENCES

1. Duret, C., and R. Pichoir in Coatings for High Temperature Applications, ed. E. Lang, Petten, Applied Science Publishers, p.33-78, (1983).
2. Morrell, P., and R. Taylor, Advances in Ceramics (Science and Technology of Zirconia III), Vol.24, p.927, (1988).
3. Morssinkhof, R.W.J., T. Fransen, and M.M.D. Heusinkveld, Materials Science and Technology, Vol.A121, p.449, (1989).
4. Coley, K.S., A.T. Tuson, S.R.J. Saunders, M.J. Bennett, and C.F. Knights, Materials Science and Technology, Vol.A121, p.461, (1989).
5. Hocking, M.G., V. Vasantasree, and P.D. Sidky, Metallic and Ceramic Coatings, Longman Scientific and Technical, New York, (1989).
6. Gesmundo, F., Proceedings of the Conference on High Temperature Materials for Power Engineering, p.67, (1990).
7. Smolinsky, G., and R.E. Dean, Materials. Letters, Vol.4, p.256, (1986).
8. Hofman, R., J.G.F. Westheim, T. Fransen, and P.J. Gellings, to be published.
9. Drory, M.D., and A.G. Evans, Journal of the American Ceramic Society, Vol.83, p.634, (1990).

10. Stott, F.H., F.M.F. Chong, and C.A. Stirling, Proceedings 9th. International Congress on Metallic Corrosion, Vol.2, p.1, (1984).
11. Rahmel, A., M. Schorr, A. Velasco-Tellez, and A. Pelton, Oxidation of Metals, Vol.27, p.199, (1987).